Luiz G. A. Martins
gustavo@facom.ufu.br
Federal University of Uberlandia
School of Computer Science
38408-100 Uberlandia, MG, Brazil

Roberto M. Finzi Neto
finzi@mecanica.ufu.br

Valder Steffen Jr.
vsteffen@mecanica.ufu.br

Lizeth V. Palomino
lvpalomino@mecanica.ufu.br

Domingos A. Rade
domingos@ufu.br

Federal University of Uberlandia
School of Mechanical Engineering
38408-100 Uberlandia, MG, Brazil

Architecture of a Remote Impedance-Based Structural Health Monitoring System for Aircraft Applications

The essence of structural health monitoring (SHM) is to develop systems based on nondestructive inspection (NDI) technologies for continuous monitoring, inspection and detection of structural damages. A new architecture of a remote SHM system based on Electromechanical Impedance (EMI) measures is described in the present contribution. The proposed environment is employed to automatically monitor the structural integrity of aircrafts and is composed by sensor networks, a signal conditioning system, a data acquisition hardware and a data processing system. The obtained results allow the accomplishment of structural condition-based maintenance strategies, in opposite to those based only on the usage time of the equipment. This approach increases the operational capacity of the structure without compromising the security of the flights. As the environment continually checks for the first signs of damage, possibly reducing or eliminating scheduled aircraft inspections, it could significantly decrease maintenance and repair expenses. Furthermore, the usage of this system allows the creation of a historical database of the aircrafts structural integrity, making possible the incremental development of a Damage Prognosis System (DPS). This work presents the proposed architecture and a set of experiments that were conducted in a representative aircraft structure (aircraft window) to demonstrate the effectiveness of the proposed system.
Keywords: *Structural Health Monitoring, Nondestructive Inspection, Electromechanical Impedance, Damage Prognosis*

Introduction

Failures occurring in industrial equipment and structures in general are associated to friction, fatigue, impact, and crack growth or to other reasons. For an appropriate functioning of the system, the failure should be localized and repaired timely. In general terms, the problem of damage monitoring consists in locating and measuring the fault and estimating the remaining life of the system. One of the most important ambitions of modern engineering is to perform structural health monitoring in real time in components of high cost and considerable responsibility. Thus, the creation or improvement of techniques that enhance the accuracy and reliability of the tracking process is highly desirable and is the subject of several studies such as the one conducted by Farrar et al. (2005).

There are several techniques for monitoring the occurrence and propagation of structural damage. One of these techniques, presented in the study of Park and Inman (2005), is the so-called Impedance-based Structural Health Monitoring (ISHM). Basically, the method, first investigated by Sun et al. (1995), identifies failures by monitoring the structure mechanical impedance that will present variations in the presence of structural damage. Since the structure mechanical impedance is difficult to obtain directly, a piezoelectric transducer, most frequently a PZT (lead-zirconate-titanate) ceramic patch bonded to the monitored structure (or embedded into it) is used as a sensor-actuator device. The electric impedance of the PZT is directly related to the mechanical impedance of the host structure, as stated in the work of Park and Inman (2005). Figure 1, first seen in the work of Raju (1997), shows the well-known one-dimensional model representation of a mechanical system containing an integrated sensor-actuator piezoelectric patch.

Nomenclature

a = *geometric constant of the PZT patch*
f_{ex} = *excitation frequency*
d_{31} = *piezoelectric coupling constant*
I_{PZT} = *current of the PZT patch*
K = *number of calculated frequency points*
N = *number of PZT ceramic patches*
PZT = *lead-zirconate-titanate ceramic patch*
V_{ex} = *excitation voltage*
Y = *electrical admittance of the PZT*
$\hat{Y}_{11}^{E}$ = *complex Young modulus*
Z = *impedance*

Greek Symbols

δ = *dielectric loss factor of the piezoelectric material*
θ = *measured phase lag between $V_{ex}(\omega)$ and $I_{PZT}(\omega)$*
ω = *angular frequency, rad/s*
ε_{33}^{T} = *dielectric constant at null stress*

Subscripts

a = *relative to the PZT mechanical impedance*
i = *relative to any of the K calculated frequency points*
j = *relative to any of the N PZT ceramic patches*
s = *relative to the structure mechanical impedance*
PZT = *relative to the PZT ceramic patch*
PZT_{Re} = *relative to the resistive part of the electrical impedance of the PZT, Ω*

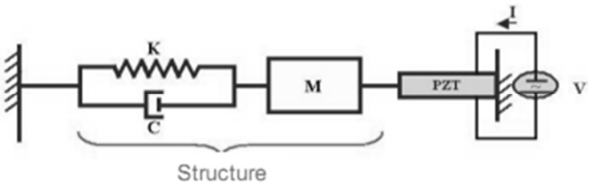

Figure 1. One-dimensional electromechanical coupling model.

Liang, Sun and Rogers (1994) stated that the solution of the wave equation for the PZT patch connected to the structure leads to a frequency-dependent, ω, is given by Eq. (1), where $Y(\omega)$ is the electrical admittance (inverse of the electrical impedance), Z_a and Z_s are the PZT mechanical impedance and the structure mechanical impedances, respectively, $\hat{Y}_{11}^{E}$ is the complex Young modulus of the PZT in the direction 1 under null electric field, d_{31} is the piezoelectric coupling constant, ε_{33}^{T} is the dielectric constant

at null stress, δ is the dielectric loss factor of the piezoelectric material, and a is a geometric constant of the PZT patch. This equation indicates that the electrical impedance of the PZT wafer bonded onto the structure is directly related to the mechanical impedance of the host structure. The electromechanical impedance over a range of frequencies is analogous to a Frequency Response Function (FRF) of the structure, which contains information regarding the structural integrity.

$$Y(\omega) = i\omega a\left[\bar{\varepsilon}_{33}^{T}(1-i\delta) - \frac{Z_s(\omega)}{Z_s(\omega)+Z_a(\omega)} d_{31}^2 \hat{Y}_{11}^2\right] \quad (1)$$

Indeed, damage causes direct changes in the structural stiffness and/or damping and alters the local dynamic characteristics of the system. As a result, $Z_S(\omega)$ uniquely determines the overall admittance of the electromechanical system, since the properties of the PZT patch remain constant. Therefore, any change in the electromechanical impedance signature is considered as an indication of structural changes, which can be induced by various types of damage.

By monitoring the measured electromechanical impedance and comparing it to a baseline measurement that corresponds to the so-called pristine condition, one can qualitatively determine that structural damage has occurred. Park and Inman (2001) confirm that the sensitivity of this technique is closely related to the frequency band selected in the excitation signal of the PZT patch. Usually, the PZT patch is excited with a sinusoidal waveform, with low amplitude (typically in the order of 1 V), but there are other studies, such as the one from Baptista et al. (2010), where higher voltages can be used with an improved sensitivity. The excitation frequencies vary from 30 kHz to 250 kHz and up to 1000 kHz for some structures and applications, as can be seen in the works of Stokes and Cloud (1993), Giurgiutiu and Zagrai (2005) and Yang et al. (2008). The optimum frequency band under practical applications remains a subject of study for the EMI-based method. Two quite interesting works about this issue are those by Peairs, Park and Inman (2004) and Peairs et al. (2006). Moura and Steffen Jr. (2006) investigated the optimal testing conditions by using meta-modeling techniques, avoiding trial-and-error approaches to determine the most suited testing conditions for a particular application.

SHM systems can play an important role in maintaining the safety of in-service structures. The development of an integrated sensory system able to monitor, collect, and deliver the information necessary for SHM becomes an important issue in this context. One of the proposed approaches is to utilize arrays of PZT patches attached to the surface of a structure or embedded in a composite material. When attached to the structure and connected to the electronics, the PZT patches become active sensors that can perform both as actuators and sensors. Thus, the impedance method allows for monitoring incipient local damage, like cracks, which produces only imperceptible and hardly noticeable changes to the large-scale dynamics of the entire structure.

A Frequency Response Function (FRF) must be obtained, for each sensor, considering at least two distinct sets. The first set of FRF represents the pristine condition of the structure and will be used as a baseline. The second set, and any future ones, will represent the actual state of the monitored structure. It is quite common to use a Fast Fourier Transform (FFT) algorithm to process the time domain measured signals so that the EMI functions in the frequency domain are obtained. The quantified difference between the FRFs, for each sensor, calculated from the pristine set and the actual state can be used to quantify a possible damage detected in the monitored structure. This assessment is traditionally made by using a scalar damage metric. The work of Palomino and Steffen (2009) presents a detailed study containing several damage metrics applied to the EMI technique that are used in the present work.

Experimental implementations of the impedance-based SHM techniques have been successfully conducted for several complex structures: the work of Chaudhry et al. (1995) presented a practical system applied to an aircraft structure with good results; Lalande et al. (1996) used the EMI technique to monitor complex precision parts; Giurgiutiu et al. (1999) achieved good results with a system used to monitor spot-welded structural joints. All these works confirm how practical an EMI system is.

Temperature changes, among all other ambient conditions, significantly affect the electric impedance signatures measured by a PZT patch. Small temperature changes cause drifts of the sensor properties and, among all these properties, the dielectric constant ε_{33}^{T} exhibits the most undesirable effect on the electrical impedance causing a baseline shift on its capacitive part. The piezoelectric coupling constant and complex Young modulus also result in baseline shift but their effect on the overall impedance is much smaller than that of the dielectric constant. The use of a modified RMSD metric, which compensates for frequency-wise and amplitude-wise shifts of the impedance function in order to minimize the temperature-induced drifts, is presented in the work of Park et al. (1999) and showed good results. Many experiments from various case studies have shown that the real part of the electromechanical impedance is sensitive enough to detect damage and other changes in the structure features than the magnitude or the imaginary part, as seen in the work of Finzi Neto et al. (2010). Thus, it can be assumed that any change in the impedance signature obtained from the PZT patch is due to changes in the mechanical impedance of the structure and the real part of the electromechanical impedance is sufficiently sensitive to exhibit those changes. But even working only with the real part it is possible that the impedance signature will be affected by temperature changes, since thermal expansion will induce small stresses in constrained structures, as demonstrated by Woon and Mitchell (1996). Moreover, the behavior of some two-part epoxy adhesives used to bond the PZT patches to the structure is also dependent on temperature changes and excitation frequency. The problem may be alleviated with the use of temperature-insensitive adhesives, as proposed by Yang, Yan, and Soh (2008). Therefore, current monitoring systems discard the imaginary part of the measured electromechanical impedance and work only with the real part to assess the monitored structures aiming at minimizing the effect of temperature changes.

This work presents a new architecture of a remote SHM system based on electromechanical impedance measurements. As previously stated, the proposed environment is employed to automatically monitor the structural integrity of aircrafts and is composed of sensor networks, signal conditioning devices, acquisition hardware and a data processing system. The next section describes the working principle and each part of the proposed system.

Mathematical Definitions of the Electromechanical Impedance

The EMI expresses a complex-valued function dependent on frequency. For each frequency, it can be represented in terms magnitude and phase. The easiest way to calculate the corresponding impedance, for a given excitation frequency, f_{ex}, is by using Eqs. (2), (3) and (4), where $V_{ex}(\omega)$ is the excitation voltage, $I_{PZT}(\omega)$ is the measured current at the excited PZT patch and θ is the measured phase lag between $V_{ex}(\omega)$ and $I_{PZT}(\omega)$.

$$|Z_{PZT}(\omega)| = \left|\frac{V_{ex}(\omega)}{I_{PZT}(\omega)}\right| \quad [\Omega] \quad (2)$$

$$\omega = 2\,\pi\, f_{ex} \quad [\text{rad/s}] \quad (3)$$

$$Z_{PZT\,Re}(\omega,\theta) = \left|\frac{V_{ex}(\omega)}{I_{PZT}(\omega)}\right| * \cos(\theta) \qquad [\Omega] \qquad (4)$$

Expanding Eq. (4) to represent a FRF containing K frequency points (i = 1, …., K), for each one of the N sensors (j = 1, …, N), results in Eq. (5).

$$Z_{PZT\,Re_j}(\omega_i,\theta_i) = \left|\frac{V_{ex_i}(\omega)}{I_{PZT_i}(\omega)}\right| * \cos(\theta_i) \qquad [\Omega] \qquad (5)$$

Equation (5) is used to calculate the FRF of the proposed system, as described in the following sections.

Signal Conditioning and Data Acquisition System

A typical impedance-based SHM system for distributed monitoring is illustrated in Fig. (2). A total of N PZT patches are bonded onto the monitored structure where each patch is connected to a Switching and Signal Conditioning System (SSCS) that will control their activation/deactivation. An external digital controller, provided by a personal computer (PC) and a digital acquisition board (DAq) or a Digital Signal Processor (DSP) module, determines the activation sequence of the PZT array. Each digital word from the controller activates only a single specific PZT patch at a time and its response is digitalized by the DAQ board and processed by the PC. A database with all baseline impedances and the new ones obtained from each PZT patch are finally processed and stored in the PC.

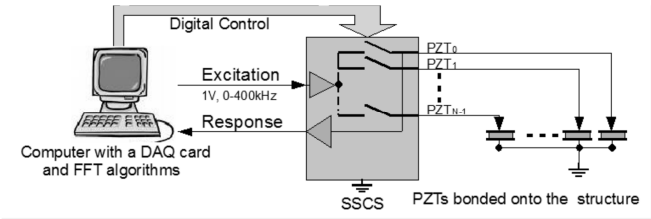

Figure 2. Typical SHM system based on monitoring the electro-mechanical impedance, for an array of PZT patches.

The acquisition system has a hybrid topology, proposed by Finzi Neto et al. (2010), in which hardware and software approaches are combined together to measure the time response signals and calculate the frequency-dependent real part of the electromechanical impedance, $Z_{PZT\,Re_j}(\omega_i,\theta_i)$, of each PZT patch j. Figure 3(a) illustrates the architecture of the hardware and Fig. 3(b) illustrates the flow chart describing how the real part of the electromechanical impedance is acquired and calculated by using a dedicated software.

The idea expressed in Fig. 3(a) is that the measures of the phase θ and the current I_{PZT} are done by dedicated hardware modules. The impedance $Z_{PZT\,Re_j}(\omega_i,\theta_i)$ $Z_{\mathrm{Re}}(\omega)$ is calculated by software, where the main advantages of this method are the following:

(a) There is no need of FFT algorithms/analyzers to generate the FRFs;

(b) I_{PZT} can be sampled at lower rates with a sampling rate independent of f_{ex} (excitation frequency);

(c) The phase θ is digitally measured by using a Two Edge Counter, which is found in any DSP. A minimum resolution of 16 bits is required for better results.

Three main circuit blocks are illustrated in Fig. 3(a):

(a) Switching System: a multiplexed array of PZT patches is a requirement for reducing costs and hardware complexity. It is quite common to use mechanical reed relays to switch the array of PZT patches, as seen in the work of Filho and Baptista (2008); however, due to their low reliability, these mechanical switches are replaced by solid state, small sized, low power consumption, and very low channel leakage devices, i.e., the so-called Analog Digitally Controlled Switches (ADCS).

(b) Signal Conditioning and Measurement: the hardware that deals with the three required parameters (V_{ex}, I_{PZT}, and θ) is concentrated in this block.

(c) DSP hardware: provides two peripherals required to conclude the impedance measurement process. The first one is a Two Edge Counter (TEC) used to measure the time t between the positive (or negative) edges of two different pulses. The second peripheral is a 16-bit Analog to Digital Converter (ADC) with at least two channels, which is used to digitalize, I_{PZT} and θ. At this point, the three parameters (V_{ex}, I_{PZT} and θ) are determined and used in Eq. (5).

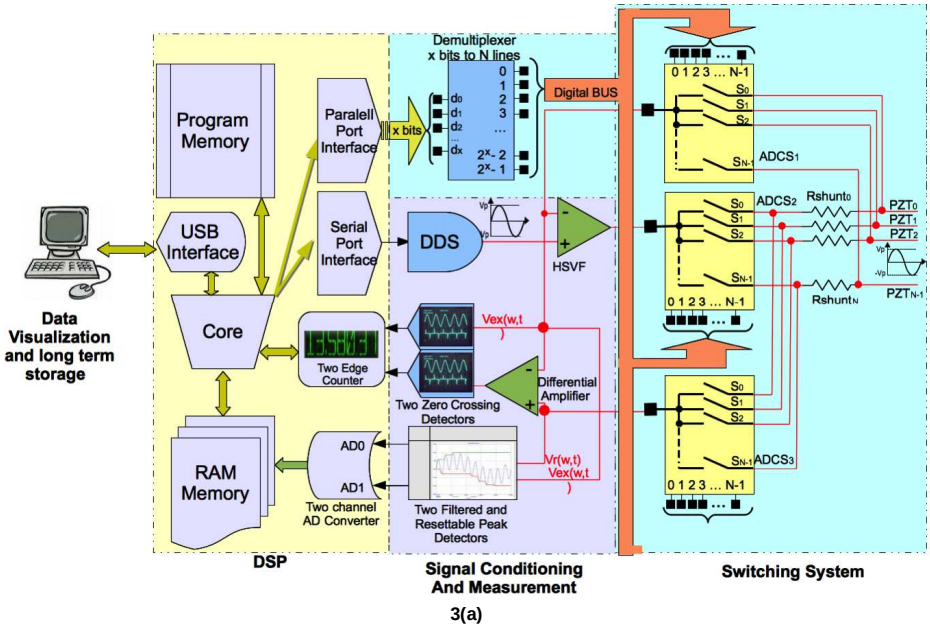

3(a)

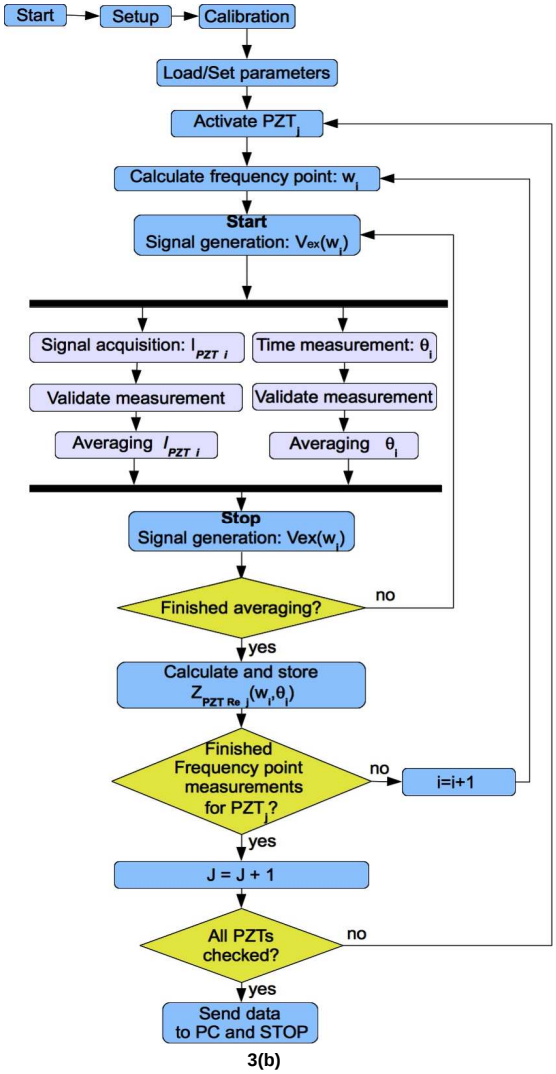

3(b)

Figure 3. SHM Acquisition System: (a) Architecture; (b) Flow chart of the DSP program.

The developed DSP software is intended to work standalone. Only a few working parameters can be recorded directly on flash memory or externally defined by a PC or other computer system through a USB connection. Figure 3(b) presents the flowchart of this computer code. The first procedure, **DSP Setup,** configures the peripherals to work properly. The next step, **Calibration,** aims at correcting any non-linearity in the generation of $V_{ex}(\omega_i)$ before any measurement is done. **Load/Set Parameters** defines the operation mode (baseline or monitoring mode), the number *j* of PZT patches in the sensing network and start/stop excitation frequency. Next, the procedure **Activated PZT$_j$** selects the next PZT, and **Calculate Frequency Point** ω_i defines the current excitation frequency. At this point, the whole system is ready to start the measurement phase. The procedure **Start Signal Generation** drives the selected PZT$_j$ with $V_{ex}(\omega_i, t)$ during the measuring process. Then, $I_{PZT\,i}$ and θ_i are measured and averaged several times so that stable values are obtained. When the averaging process is finished, $Z_{PZT_{Re\,j}}(\omega_i, \theta_i)$ is calculated and stored in the memory.

The prototype of the acquisition system can be observed in Fig. 4. The Acquisition System can be seen on the left and the DSP module is seen on the right. A multi-wire shielded cable connects both circuits. Due to the architecture presented in Fig. 3, the length of this cable is not an issue for long distance measurements. Experimental results, using a cable of 40 meters, were conducted successfully.

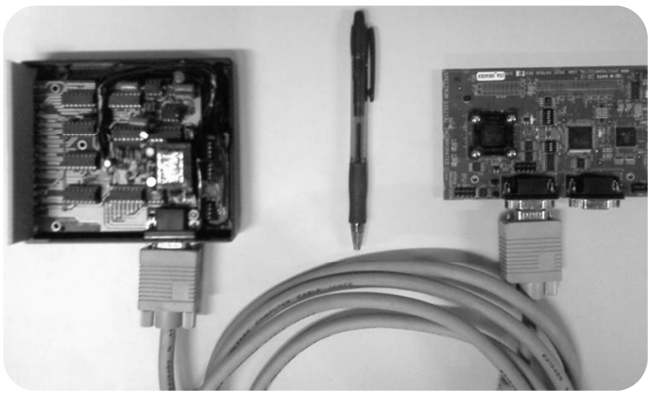

Figure 4. Illustration of the prototype.

Remote Data Processing

The off-line SHM system operation depends on the communication between the embedded environment, which is responsible for the signal acquisition, and the server environment (aircraft manufacturer) that carries out the data analysis. Figure 5 presents a simplified architecture of the proposed system communication platform.

The essence of the embedded system functionality comprises the download of the configuration files, the set of FRFs obtained from the Signal Acquisition Module and the periodic exchange of files between the embedded and the server environments through a safe internet connection using the SFTP (SSH File Transfer Protocol) containing a user authentication device and public key-based cryptography. The signal acquisition module performs both the checking of the sensor network status and the control, captures and stores the data related to the monitored aircraft structure state at chosen time instants. The transfer module is responsible for the communication with the server environment, performing the data files upload and the configuration files download. The configuration files use XML (Extensible Markup Language) file format, which assures a standardized information exchange and, consequently, the possible employment of other monitoring techniques in the future, without requiring changes in the communication process.

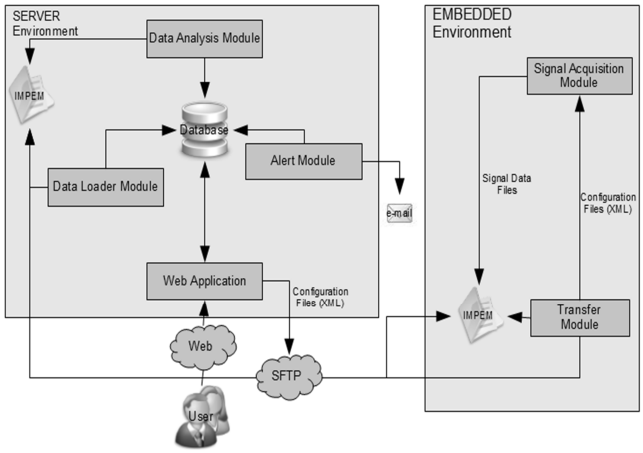

Figure 5. Software and communication platform for the remote off-line SHM system.

The server environment is responsible for loading the data files to the system database; analyzing and storing the damage data and the analyses results; sending alerts when damage is detected; interfacing the user and the monitoring system. This interface is related to the system front-end and is composed of Internet applications, which were conceived to allow remote user interactions. The data analysis module identifies and analyzes the pending test registers from the database, in accordance with established criteria. The analysis is performed for each transducer by comparing the corresponding data with those from the respective baseline. The analysis consists in the consolidation of the values obtained from using the previously defined damage metrics in accordance with the adopted configuration (e.g. sensitivity factors, damage threshold and metric weights), which is also registered in the database. This process permits the creation of a historical database of the aircraft structural integrity, which should be used in the incremental development of a Damage Prognosis System (DPS). When structural damages are detected, the alert module sends a standardized e-mail message to previously defined users.

Almost the entire system operates automatically; however, some operations (system configuration, for example) need interaction between the monitoring system and the user. In these cases, it is fundamental that the system resources and functionalities be available both by physical access to the instruments that encompass the monitoring system and by remote access through a web browser. Therefore, techniques, languages and development tools were employed aiming at creating web-based solutions (Internet or Intranet), which make possible remote access for users previously stored in the database. This Web solution was developed by using the RIA (Rich Internet Applications) approach, i.e., web applications with characteristics and functionalities such as a customer-server solution. Traditional RIAs transfer the application processing to the Internet browser, but keep most of the data in the application server. The proposed web application provides a graphical interface to the user for administration purposes (configuration and maintenance) and also for visualization of the analyses details.

Damage Metrics Computation

The analysis process is managed by some configuration parameters that are previously defined. Eight damage metrics were chosen to be used during the analysis. Four of these are variations of the most used statistical model found in the work of Palomino and Steffen (2009), the so-called root square mean deviation (RSMD). The other damage metrics are the correlation coefficient deviation (CCD), the average square difference (ASD), the mean absolute percentage deviation (MAPD) and the sum of the average difference between the signals (M). These metrics can be combined or can be used individually, in accordance with the adopted configuration for the analysis.

The damage metric computations are carried out for each PZT patch involved in the monitoring. Since the acquisition cycle encompasses H measurements, each metric computation deals with $2H$ values. Half of them are related to baseline signals and the other half are related to the current signal acquired. After the computation, the metric values are consolidated for each sensor considered in order to determine the probability of damage existence. Basically, the damage detection is evaluated by analyzing the metric values differences resulting from the comparison between current signals and baseline signals. Usually damage detection is performed manually through the comparison of the metric values obtained both from the current and baseline signals. In the analysis module, an automatic method for damage detection was designed. This method defines the existence of damage based on damage metric mean values and their corresponding standard deviations calculated from measurements collected from each sensor (current and baseline signals). Finally, damage detection is performed for each one of the damage metrics considered and each sensor installed in the structure by using the following decision criteria:

1. The PZT patches presenting high standard deviations are rejected and discarded from the analysis.
2. If all damage metric values obtained for the PZT patches included in the analysis are lower than a given minimum value established for each damage metric considered, it is assumed that no damage has occurred.
3. If some of the damage metric values obtained from the PZT patches are higher than a given minimum value established for each one of the damage metrics, the standard deviations are used to define if the corresponding damage metrics effectively detected damage.
4. If some standard deviations are close to zero, the mean values of the damage metrics are used to define if the corresponding damage metrics effectively detected damage.
5. The values of the damage metrics calculated for the PZT patches that have been included in the analysis are compared to each other to determine if the variations of these values are significant.

Then, the results corresponding to the damage metrics are consolidated to obtain a damage indicator for each sensor employed in the monitoring. This damage indicator is calculated through a weighted mean of the damage metrics values as follows:

$$PF_j = \frac{\sum_{h=1}^{m} W_h R_{h\,j}}{\sum_{h=1}^{m} W_h} \tag{6}$$

where PF_j is the damage indicator of the sensor j; m is the number of metrics used in the analysis; $R_{h\,j}$ is the damage metric value obtained for the h^{th} metric and j^{th} sensor; and W_h is the weight associated to the metric h. This weight defines the influence of the metric on the structural damage determination.

The indication of damage detection is considered as positive when the corresponding damage probability is larger than the threshold value previously specified in the system configuration. The case study presented in the next session defines this threshold at 0.80.

Case Study: Aluminium Aircraft Panel

The experiment was conducted at room temperature in the reinforced fuselage panel showed in Fig. 6(a). Due to the size and complexity of the structure, ten PZT patches were used in the experiment. Six square PZT patches were bonded to the trusses and four circular PZT patches were bonded to the plate, as seen in Fig. 6(b). The number of PZT patches used was arbitrary and no preliminary study was done to optimize this number. Six tests were performed to check the performance of the damage detection system. The first test was dedicated to the baseline, the second one was made for the case without damage, and the next four tests were performed after the inclusion of simulated damages, as shown in Fig. 6(c). The damage inserted sequentially in the tests #3 to #6 was not removed from the system for the next tests, so that the test #6 accumulates four damages.

The results obtained for the system can be observed in Fig. 7. The first test was taken as being the baseline. No damage was added to the second test. Thus, the light signals of the monitoring system were off (Fig. 7(a)). In test #3, when a mass was added close to PZT3, the system evidenced the damage through a light signal at the position corresponding to PZT3 (Fig. 7(b)). In test #4, the mass added close to

PZT3 was kept and another mass was added close to PZT9 (Fig. 7(c)). In the next test (test #5), the two masses were kept and the clamp located close to PZT7 was removed. As observed for the previous cases the damage was satisfactorily detected by the system (Fig. 7d). In the last test, all damages inserted in the structure were kept and the clamp located close to PZT9 was removed. As one of the masses was close to PZT9, this PZT was already activated.

(a)

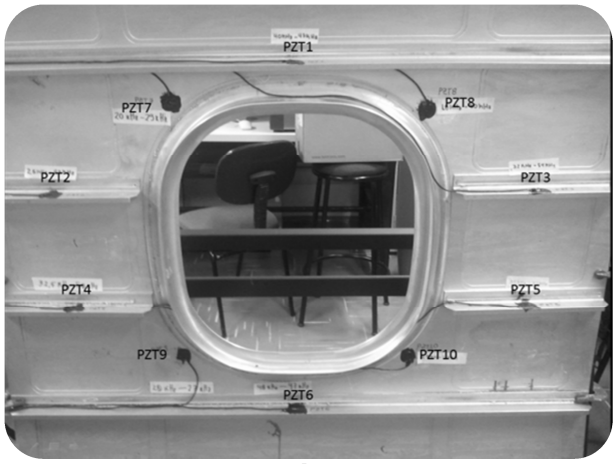

(b)

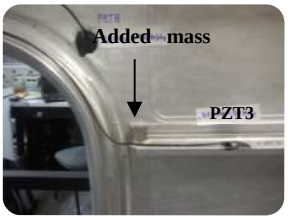

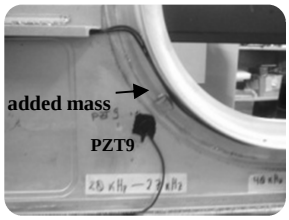

Test 3 Test 4

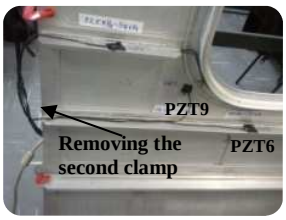

Test 5 Test 6

(c)

Figure 6. (a) Aircraft window; (b) detail of the ten PZT patches; (c) detail of the damages inserted.

(a)

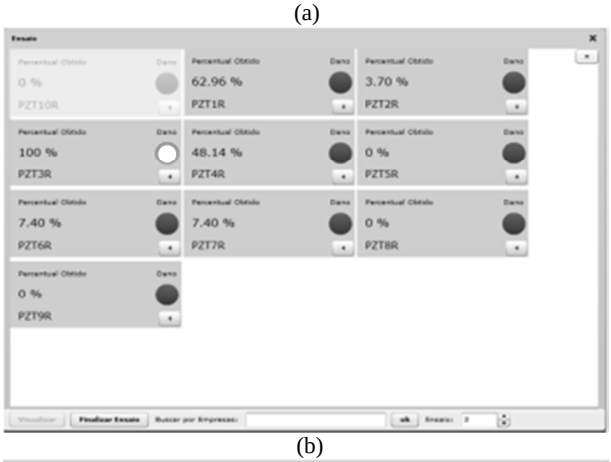

(b)

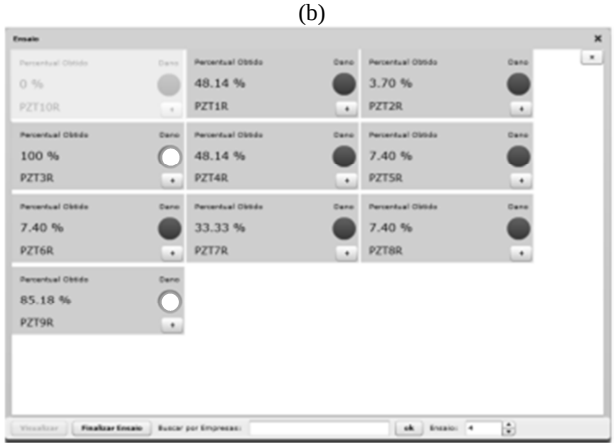

(c)

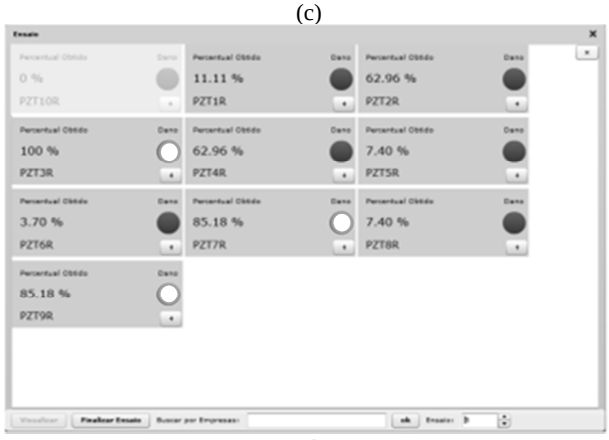

(d)

(e)

Figure 7. Monitoring results: (a) Test #2; (b) Test #3; (c) Test #4; (d) Test #5; (e) Test #6.

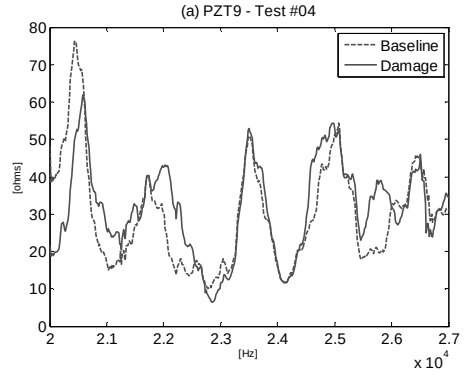

(a)

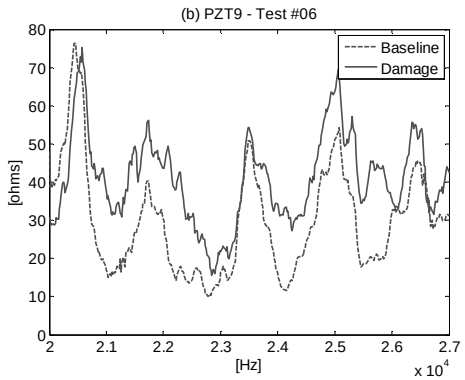

(b)

Figure 8. Variations of the signal from PZT9. (a) Test #4; (b) Test #6.

Figure 8 presents the variations of the signals from PZT9 corresponding to two damage configurations together (an added mass and a removed clamp). The difference between the baseline signal and the damage signal in each state is clear.

In all tests the PZT10 was disabled, since it presented an excessively large standard deviation. Further investigation identified a bad coupling between the structure and this PZT patch. A probable reason for that may be a non-uniform layer of adhesive applied or some defect in the PZT patch. Either way, the system correctly disregarded the information from this sensor.

Conclusion

In this article, a new architecture for a remote SHM system based on the electromechanical impedance technique was described. The proposed environment is employed to automatically monitor the structural integrity of aircrafts and is composed of sensor networks, signal acquisition system and data processing system. The sensor networks together with the signal acquisition system capture the data related to the monitored aircraft structure state at chosen time instants. Collected data are sent to the data processing system, which performs the analysis to identify and locate possible damages. A real world (aluminium aircraft reinforced panel) case study was presented and the results were found to be satisfactory in the damage detection procedure. The obtained results allow the accomplishment of structural condition-based maintenance strategies, as opposed to those based only on the usage time of the equipment (periodic maintenance). This approach increases the operational capacity of the structure without neglecting the security of the flight in the case of real applications. As the system continually checks for incipient damage, the need for scheduled aircraft inspections can be reduced, thus significantly decreasing maintenance and repair expenses. Furthermore, the use of the proposed monitoring system permits the creation of a historical database regarding the structural integrity of aircrafts, making possible the incremental development of a Damage Prognosis System (DPS). Such DPS is used to predict the remaining life of structural systems.

Acknowledgement

The fourth author is thankful to CNPQ for her DSc scholarship. The authors are grateful to FAPEMIG and CNPq for partially funding this research work through INCT-EIE.

References

Baptista, F.G, Filho, J.V., and Inman, D.J., 2010, "Influence of Excitation Signal on Impedance-based Structural Health Monitoring", *Journal of Intelligent Material Systems and Structures*, 21(9), pp.1409-1416.

Chaudhry, Z., Joseph, T., Sun, P. and Rogers C., 1995, "Local-Area Health Monitoring of Aircraft via Piezoelectric Actuator/Sensor Patches". Smart Structures and Integrated Systems, SPIE Conference, Proceedings of the SPIE, San Diego-USA.

Farrar, C.R., Lieven, N.A.J. and Bement, M.T., 2005, "An Introduction to Damage Prognosis", Damage Prognosis for Aerospace, Civil and Mechanical System, Wiley, Cap.1, pp. 1-12.

Filho, J. and Baptista, F.A., 2008, "New Impedance Measurement System for PZT Based Structural Health Monitoring", *IEEE Transactions on Instrumentation & Measurements*, Vol. 58, No. 10, pp. 3602-3608.

Giurgiutiu, V., Reynolds, A. and Rogers, C.A., 1999, "Experimental investigation of E/M impedance health monitoring of spot-welded structural joints", *Journal of Intelligent Materials System Structures*, 10, pp. 802-812.

Finzi Neto, R.M., Steffen Jr., V., Rade, D.A., Gallo, C.A. and Palomino, L.V., 2010, "A low-cost electromechanical impedance-based SHM architecture for multiplexed piezoceramic actuators", *Journal of Structural Health Monitoring*, DOI:10.1177/1475921710379518.

Giurgiutiu, V. and Zagrai, A.N., 2005, "Damage detection in thin plates and aerospace structures with the electro-mechanical impedance method", *Journal of Structural Health Monitoring*, 4, pp. 99-118.

Lalande, F., Childs, B., Chaudhry, Z. and Rogers C.A., 1996, "High-frequency impedance analysis for NDE of complex precision parts". In: Proceedings of SPIE Conference on Smart Structures and Materials, Vol. 2717, San Diego, CA, SPIE Publishing, pp. 237-245.

Liang, C., Sun, F.P. and Rogers, C.A., 1994, "Coupled Electromechanical Analysis of Adaptive Material Systems – Determination of the Actuator Power Consumption and System Energy Transfer", *Journal of Intelligent Material Systems and Structures*, 5, pp. 12-20.

Moura Jr, J.R.V and Steffen Jr, V. (2006). "Impedance-Based Health Monitoring for Aeronautic Structures using Statistical Meta-modeling", *Journal of Intelligent Material Systems and Structures*, Vol. 17, pp. 1023-1036.

Palomino, L.V. and Steffen, V., 2009, "Damage Metrics Associated with electromechanical Impedance Technique for SHM Applied to a Riveted Structure", Proceedings of COBEM2009 20th International Congress of Mechanical Engineering, Gramado-Brazil.

Park, G., Kabeya, K., Cudney, H.H. and Inman, D.J., 1999, "Impedance-based structural health monitoring for temperature varying applications". *JSME Int. J*., Ser A, 42(2), pp. 249-258.

Park, G. and Inman, D.J., 2001, "Impedance-based structural health monitoring", monograph: In: Woo, S.C. (ed), Nondestructive Testing and Evaluation Methods for Infrastructure Condition Assessment, New York, NY: Kluwer Academic Publishers.

Park, G. and Inman, D.J., 2005, "Impedance-Based Structural Health Monitoring", Damage Prognosis for Aerospace, Civil and Mechanical System, Wiley, Cap.13, pp. 1-12.

Peairs D.M., Park G. and Inman, D.J., 2004, "Improving accessibility of the impedance-based structural health monitoring method", *J. Intell. Mater. Syst. Struct*., 15(2), pp. 129-139.

Peairs D.M., Tarazaga P.A. and Inman, D.J., 2006, "A study of the correlation between PZT and MFC resonance peaks and damage detection frequency intervals using the impedance method", International Conference on Noise and Vibration Engineering, Leuven, Belgium, 18-20 September 2006, pp. 909-924.

Raju, V., 1997, "Implementing Impedance-Based Health Monitoring", MSc Thesis, Virginia Tech, USA.

Sun, F.P., Chaudhy, Z., Liang, C. and Rogers, C.A., 1995, "Truss Structure Integrity Identification Using PZT Sensor – Actuator", *Journal of Intelligent Material Systems and Structures*, 6, pp. 134-139.

Stokes, J.P. and Cloud, G.L., 1993, "The application of interferonmetric techniques to the nondestructive inspection of fiber-reinforced materials", *Experimental Mechanics*, 33, pp. 314-319.

Woon, C.E. and Mitchell, L.D., 1996, "Variations in structural dynamic characteristics caused by changes in ambient temperature: Part II." In: Analytical, Proceedings of 14th International Modal Analysis Conference, Dearborn, MI, 12-15 February 1996, SEM, pp. 972-980.

Yang, Y., Yan, Y. and Soh, C.K., 2008, "Practical issues related to the application of the electromechanical impedance technique in the structural health monitoring of civil structures: I. Experiment", *Smart Materials and Structures*, 17035008 (14pp).